Glycoprotein Ib clustering in platelets can be inhibited by alpha-linolenic acid as revealed by cryo-electron tomography

Stivala, Simona ; Sorrentino, Simona ; Gobbato, Sara ; Bonetti, Nicole R ; Camici, Giovanni G ; Lüscher, Thomas F ; Medalia, Ohad ; Beer, Jürg H

Abstract: Platelet adhesion to the sub-endothelial matrix and damaged endothelium occurs through a multi-step process mediated in the initial phase by glycoprotein Ib binding to von Willebrand factor, which leads to the subsequent formation of a platelet plug. The plant-derived omega-3 fatty acid alpha-linolenic acid is an abundant alternative to fish-derived n-3 FA and has anti-inflammatory and anti-thrombotic properties. In this study, we investigated the impact of alpha-linolenic acid on human platelet binding to vWF under high-shear flow conditions (mimicking blood flow in stenosed arteries). Pre-incubation of fresh human blood from healthy donors with alpha-linolenic acid at dietary relevant concentrations reduced platelet binding and rolling on vWF-coated microchannels at a shear rate of 100 dyn/cm2. Depletion of membrane cholesterol by incubation of platelet-rich-plasma with methyl-beta cyclodextrin abrogated platelet rolling on vWF. Analysis of glycoprotein Ib by applying cryo-electron tomography to intact platelets revealed local clusters of glycoprotein Ib complexes, upon shear-force exposure, whose formation could be prevented by alpha-linolenic acid treatment. This study provides novel findings on the rapid local rearrangement of the glycoprotein Ib complexes in response to high-shear flow and highlights the mechanism of in vitro inhibition of platelet binding to and rolling on vWF by alpha-linolenic acid.

DOI: https://doi.org/10.3324/haematol.2019.220988

haematologica
Journal of The Ferrata Storti Foundation

Glycoprotein Ib clustering in platelets can be inhibited by alpha-linolenic acid as revealed by cryo-electron tomography

by Simona Stivala, Simona Sorrentino, Sara Gobbato, Nicole R. Bonetti, Giovanni G. Camici, Thomas F. Lüscher, Ohad Medalia, and Jürg H. Beer

Haematologica 2019 [Epub ahead of print]

Citation: Simona Stivala, Simona Sorrentino, Sara Gobbato, Nicole R. Bonetti, Giovanni G. Camici, Thomas F. Lüscher, Ohad Medalia, and Jürg H. Beer. Glycoprotein Ib clustering in platelets can be inhibited by alpha-linolenic acid as revealed by cryo-electron tomography.
Haematologica. 2019; 104:xxx
doi:10.3324/haematol.2019.220988

Glycoprotein Ib clustering in platelets can be inhibited by alpha-linolenic acid as revealed by cryo-electron tomography

Simona Stivala[1], Simona Sorrentino[2], Sara Gobbato[1], Nicole R. Bonetti[1,3], Giovanni G. Camici[1,4,5], Thomas F. Lüscher[1], Ohad Medalia[2,6] and Jürg H. Beer[1,3]

[1] *Laboratory for Platelet Research, Center for Molecular Cardiology, University of Zurich, Zurich, Switzerland;*

[2] *Department of Biochemistry, University of Zurich, Zurich, Switzerland;*

[3] *Internal Medicine, Cantonal Hospital of Baden, Baden, Switzerland;*

[4] *University Heart Center, University Hospital Zurich, Switzerland;*

[5] *Department of Research and Education, University Hospital Zurich, Switzerland.*

[6] *Department of Life Sciences and the National Institute for Biotechnology in the Negev, Ben-Gurion University, 84105 Beer-Sheva, Israel*

Simona Stivala and Simona Sorrentino contributed equally to this work

Running head: GpIb clustering in shear-activated platelets

Corresponding author:

Jürg H. Beer

Laboratory for Platelet Research, Center for Molecular Cardiology, University of Zurich

and Cantonal Hospital of Baden, Internal Medicine

Im Ergel, 1, 5404 Baden, Switzerland

Phone: (++41) 56 486 25 02; Fax: (++41) 56 486 25 09

E-mail: hansjuerg.beer@ksb.ch

Total Word Count: 2338; Abstract: 199; Figures: 5; Supplemental Data files: 3.

Abstract

Platelet adhesion to the sub-endothelial matrix and damaged endothelium occurs through a multi-step process mediated in the initial phase by glycoprotein Ib binding to von Willebrand factor, which leads to the subsequent formation of a platelet plug. The plant-derived omega-3 fatty acid alpha-linolenic acid is an abundant alternative to fish-derived n-3 FA and has anti-inflammatory and anti-thrombotic properties. In this study, we investigated the impact of alpha-linolenic acid on human platelet binding to vWF under high-shear flow conditions (mimicking blood flow in stenosed arteries). Pre-incubation of fresh human blood from healthy donors with alpha-linolenic acid at dietary relevant concentrations reduced platelet binding and rolling on vWF-coated microchannels at a shear rate of 100 dyn/cm^2. Depletion of membrane cholesterol by incubation of platelet-rich-plasma with methyl-beta cyclodextrin abrogated platelet rolling on vWF. Analysis of glycoprotein Ib by applying cryo-electron tomography to intact platelets revealed local clusters of glycoprotein Ib complexes, upon shear-force exposure, whose formation could be prevented by alpha-linolenic acid treatment. This study provides novel findings on the rapid local rearrangement of the glycoprotein Ib complexes in response to high-shear flow and highlights the mechanism of in vitro inhibition of platelet binding to and rolling on vWF by alpha-linolenic acid.

Introduction

The first event leading to the formation of a platelet plug is mediated by the glycoprotein Ib-IX complex (GpIb-IX), the second most-abundant platelet receptor after the integrin αIIbβ3[1–3]. Platelet binding to von Willebrand factor (vWF) is tightly controlled in order to occur only at sites of bleeding but not in the normal circulation, where it would cause thrombosis. This regulation involves activation of vWF only at high flow rates and binding of GpIb to the A1 domain of vWF through a 2-step mechanism, where vWF multimer first elongates, then the A1 domain transitions to a high-affinity state[4–6]. The role of high-shear flow in the pathogenesis of thrombosis is particularly relevant under pathological conditions such as in stenosed, atherosclerotic arteries, where shear stress can increase above 100 dyn/cm^2 (shear rate > 4000/sec)[7,8]. Because of its pivotal role in initiating platelet adhesion, GpIb represents a promising anti-thrombotic target.

Omega-3 fatty acids (n-3 FA) are a class of naturally occurring polyunsaturated fatty acids; the plant-derived alpha-linolenic acid (ALA), whose cardioprotective effects have been shown by us and others[9–12], is readily available, whereas limited fishery resources and sea pollution restrict the use of marine-derived n-3 FA[13–15]. N-3 FA modulate cellular responses through incorporation into plasma membranes and reduction in the formation of typical protein complexes/lipid rafts, among other effects[16–18]. Based on our previous observations that ALA reduces platelet reactivity[10,19], and on studies showing the presence of GpIb in lipid rafts[20–22], we hypothesized that ALA might interfere with GpIb distribution on the plasma membrane in high-shear flow and, therefore, binding to vWF.

Methods

Blood samples

Blood from healthy volunteers was obtained from the Blood Center of the Swiss Red Cross at the Cantonal Hospital Baden with informed consent according to the declaration of Helsinki. The study was approved by the Institutional Review Board. EDTA or citrated blood was kept at room temperature until assays performed (within 2 hours of drawing). Blood was incubated with vehicle (0.1% ethanol) or ALA 30 μM for 1 hour at room temperature before being used for subsequent experiments. The n-3 FA dose was chosen based on a previous study showing this to be a dietary reachable concentration[23] . Platelet adhesion to vWF was performed on a Bioflux 200 system (Fluxion Bioscience, San Francisco, US) according to the manufacturer's protocol (see Supplementary Data file for details).

Immunofluorescence staining for Ground State Depletion (GSD) microscopy

Washed platelets isolated from vehicle or ALA-treated samples were fixed with 4% PFA for 15 minutes, then spun on a 1.5 coverslip in a Cytospin (Thermo Fisher Scientific, Waltham, US) and stained for GSD microscopy. For details, see the Supplementary Data file.

Flow cytometric analysis of vWF binding

Platelet-rich plasma (PRP) or washed platelets from vehicle or ALA-treated blood samples were fixed with 4%PFA for 15 minutes, followed by incubation in 1%BSA in PBS containing a rabbit anti-human vWF antibody (1:500, Dako A0082) and an anti-GpIbα-APC (BD Bioscience, San Jose, US) for 1 hour. In some experiments, exogenous human vWF (100 ug/ml, Hematologic Technologies) was added to washed platelets. Samples were washed 3x in 1% BSA in PBS and then stained with an anti-rabbit 488 (1:250, Jackson Immunoresearch, West Grove, PA, USA) for 30 minutes. After 3 washes in 1% BSA in PBS, samples were resuspended in 300 µl PBS and analyzed on a LSR Fortessa (BD Bioscience, San Jose, US).

Cryo-electron tomography

Resting and sheared platelets in Tyrode's buffer were seeded on gold grids coated with a Silicon mesh (R 1/4, 200 mesh, Quantifoil, Jena, Germany). Platelets were allowed to adhere for 10 min and then fixed with 4% formaldehyde for 5 min at room temperature, before being processed for cryo-electron tomography. Receptor detection was achieved for GpIb and integrin αIIbβ3 with immunogold labeling (details are given in the Supplementary Data). Data acquisition was performed using an FEI Titan Krios. Tomograms were acquired with a magnification of 42,000× corresponding to a pixel size of 0.34 nm. The receptors density was analyzed using MATLAB scripts and the receptors distributions were plotted and statistically analyzed by the OriginLab software (Northampton, Massachusetts, USA).

Statistical analysis

Data are plotted as mean ±SEM of at least three independent experiments. They were analysed by paired, two-tailed Student's t-test with GraphPad Prism version 7 (GraphPad Software, La Jolla, US). *P* values <0.05 were considered significant.

Results

Pre-incubation of blood with the n-3 FA ALA at dietary relevant concentrations[23] reduced GpIb/vWF interaction under pathological high-shear flow (10'000 s-1, corresponding to an 80% stenosed artery), as measured by the platelet-covered area (106'963 ±15'892 μm^2 vehicle vs 75'519 ±16'254 μm^2 ALA, Figure 1A-B and Supplemental Video 1 and 2). Analysis of single fluorescently labelled platelets showed that their speed was doubled when pre-incubated with ALA (Figure 1C), while the distance travelled before stopping was increased (8.89 ±4.0 µm vehicle vs 13.36 ±7.2 µm ALA, Figure 1D and E).

It has been reported that GpIb resides in cholesterol-rich membrane domains termed lipid rafts[20,21,24,25], and that it appears to cluster in high-shear flow conditions[22]. In agreement with these findings, cholesterol depletion with methyl-beta-cyclodextrin (MβCD), able to remove 50-90% of membrane cholesterol[26], greatly reduced platelet adhesions to vWF, demonstrating the pivotal role of membrane cholesterol in GpIb-vWF adhesion under high-shear flow (188±16 μm^2, Figure 1F).

To exclude that the reduced adhesion of ALA-treated platelets was due to lower levels of membrane GpIb, vehicle and ALA-treated washed platelets were exposed to high-shear flow in a viscometer (10'000 s^{-1}, 1 minute) and analysed by flow cytometry. Levels of membrane GpIb were not different between vehicle and ALA-treated platelets (Figure 2A); rather, pre-treatment with the n-3 FA preserved GpIb levels, as shown by higher fluorescence values, suggesting it had an inhibitory effect on GpIb cleavage, as previously shown by our group[19].

Next, we analysed whether the effect on GpIb-vWF binding was specific for GpIb, vWF, or both. Whole blood was pre-treated with ALA or vehicle for 1 hour, followed by isolation of platelet-rich plasma (PRP) and exposure to high-shear flow (10'000 s^{-1}, 1 minute). Flow cytometric analysis of platelet-bound vWF showed that pathological high-shear flow was able to induce GpIb-vWF binding, and that this was not influenced by the presence of ALA (Figure 2B). When the same experiment was performed with washed platelets, we could not detect any platelet-bound vWF, demonstrating the plasmatic origin of the bound vWF (Figure 2C); however, addition of exogenous human vWF to washed platelets was able to restore vWF-platelet binding (Figure 2C). These results show that ALA has no effect on vWF itself, and suggest that its inhibitory effect is exerted through platelet GpIb and is specific for binding to anchored vWF (as typically exposed *in vivo* from endothelial cells after injury).

High resolution imaging of the GpIb receptors at the plasma membrane of intact platelets was conducted using cryo-electron tomography[27] (cryo-ET, Figure 3 A-C). Adherent platelets were incubated with anti-GpIb antibodies decorated with 6-nm gold-protein A and imaged with cryo-ET. The coordinates of the gold nanoclusters were identified (Figure 3 A-C). While the overall number of receptors per platelet is not significantly varied (115 ±50 per μm^2 for the adherent platelets and 130 ±50 per μm^2 in the case of the sheared activated platelets), the distribution of receptors varied. To quantify these changes, we analysed the clustering properties of GpIbα by calculating, for each receptor, the number of receptors within a 50 nm radius. Figure 3 E-G shows normal distributions of neighbourhood receptors, with an average of 2.5 ± 1.8 neighbours for the adherent platelets, 3 ± 2.3 neighbours for the shear activated platelets and 3 ± 1.8 in the case of the ALA treated platelets. While the global distribution of receptors remains similar, 9% of the receptors have ≥12 neighbours in the shear activated platelets (41/453, Figure 3F), while in the case of platelets treated with ALA only 3.8% of receptors have more than 12 neighbours (14/366, Figure 3G). As a control, we have analysed the density and number of neighbours of the platelet integrin αIIbβ3. This analysis showed a much higher density of the integrin receptors (450 ± 180 per μm^2) and with many neighbours in comparison to the GpIb receptors (10 ± 5, Figure 3 D and H, and Supplementary Figure 3), which is in agreement with the difference in abundance of the two receptors in platelets[28].

Analysis of immunofluorescent-stained GpIbα by GSD super-resolution microscopy also revealed that GpIb is abundantly expressed over the whole platelet membrane with small local points of high density (Figure 4A). To compare between the GSD microscopy and cryo-ET we have adopted a recently developed strategy[29]. We used an assembly of the cryo-ET data into a 5 µm x 5 µm collage, where the coordinates of the 6 nm gold labeled GpIb were drawn as red dots and blurred to 20 nm resolution to match the GSD data (Figure 4B). The obtained synthetic model of platelet perimeter shows a distribution and appearance of the receptor in agreement with the fluorescence data, with high density of GpIb throughout the membrane, but, interestingly, also local, small regions of more densely packed complexes (Figure 4B, arrowhead). Blood pre-treatment with ALA did not show a change in the distribution of membrane GpIb by total internal reflection fluorescence (TIRF), likely due to the small size of GpIb clusters, which is in the same range of the resolution of the technique (Figure 5).

Discussion

α-Linolenic acid is a plant-derived n-3 FA readily available in certain plant oils such as flaxseed, soybean and canola oil. Epidemiological studies have shown an inverse correlation between dietary ALA and cardiovascular events[11,30,31], although the molecular mechanisms of this protection are not completely known. Our group has investigated the molecular basis of several cardio-protective effects of ALA, showing that at least some of its effects are mediated by its action on endothelial cells, leukocytes and platelets[9,10,19]. In this study, we have focused in particular on platelet adhesion to vWF under high-shear conditions, which represents the first step mediating platelet activation under arterial flow and is especially important in stenosed (atherosclerotic) arteries, where shear can reach extremely high values (>5'000 s^{-1})[7,32,33].

Here we show for the first time that ALA is able to partially inhibit platelet adhesion to vWF under a shear flow of 10'000 s^{-1}, when whole blood is pre-incubated for 1 hour with ALA at dietary relevant concentrations[23]. This is accompanied by an increase in speed and distance traveled by ALA-treated platelets, compared to vehicle treatment (Figure 1), and extends previous results from our group showing a reduced aggregation of citrate platelets over collagen at low shear[19] . The effect observed is specific to anchored vWF, since vWF binding upon exposure of platelet-rich plasm to high-shear flow could not be altered by ALA pre-treatment (Figure 2). A similar inhibition of platelet adhesion is obtained with the longer, marine-derived n-3 FA eicosapentaenoic acid (EPA), while the saturated fatty acid stearic acid had no effect (Supplementary Figure 4). Although the inhibitory effect of ALA may seem small (25% reduction in platelet adhesion), its biological implications are important, since inhibition at this early step will reduce the number of platelets activated in response to GpIb engagement and subsequent signaling leading to thrombus formation. The additional inhibitory effects of ALA at the level of intracellular signaling and granule secretion will lead, overall, to a greater effect with a relevant biological significance on atherothrombosis.

Since platelet binding to vWF is mediated by the GpIb receptor, we employed state-of-the-art methods (superresolution microscopy by GSD and cryo-electron tomography) to analyze GpIb distribution on the platelet membrane at high-resolution.

The GpIb distribution analysis by cryo-ET suggests that a significant subpopulation of receptors clustered into a high number of neighbours in the shear activated (and to a lesser extent in the ALA-treated) platelets, indicating that platelet exposure to shear stress induces a

local rearrangement of GpIb at the platelet plasma membrane, forming discrete small regions of high receptor density (Figure 3). These regions presumably represent high affinity "binding units" or even binding loci for anchoring of multimeric vWF.

Our observations are in line with previous findings[34] showing that under high-shear stress platelets form local points of adhesion, termed "discrete adhesion points" (DAPs), and describing DAPs as the putative regions of interaction between platelets/vWF. Our functional and structural data provides a high-resolution insight into the position of the GpIb receptors and supports a model where high-shear stress induces a rapid, local rearrangement of GpIb receptors into small "clusters" of 15-20 complexes. This subpopulation of receptors may represent the previously described high-affinity binding units that interact with vWF and enable platelet rolling under arterial flow. Pre-incubation of platelets with ALA reduces the local clustering of GpIb receptors as shown by the virtual absence of larger complexes (GPIb with ≥17 neighbors, Figure 3C and G). On the functional side, this provides an explanation as to why adhesion is significantly inhibited by ALA pre-treatment while platelet rolling speed is increased (Figure 1A and C). Previous work has shown that omega-3 (of marine origin) can inhibit protein palmitoylation and, therefore, localization to lipid rafts[35]. Although in our settings we have used a pre-incubation time too short to achieve an analogue effect, long-term, nutritional supplementation with ALA may also inhibit GpIb localization to lipid rafts via a reduced palmitoylation and, consequently, reduce platelet adhesion to vWF even more through this additional mechanism.

Taken together, these data provide insight into the possible mechanism of the anti-thrombotic properties of n-3 FA in the early phase of thrombosis at sites of arterial stenosis or plaque. It may therefore represent the basis for a therapeutic approach which interferes with this process.

In conclusion, our structural data from intact platelets, including cryo-ET and super-resolution microscopy, show that upon high-shear conditions platelet GpIb receptors reorganize into "clusters" of 10 to 20 complexes closer to each other than on resting platelets; functionally, we demonstrate that - by the intervention with the plant-derived n-3 FA ALA - the size of these clusters is reduced, thereby reducing platelet adhesion to vWF under high-shear flow. This highlights its potential as an anti-thrombotic agent.

Acknowledgements

This work was supported by a grant from the Swiss National Foundation of Science, the Swiss Heart Foundation, the Kardio Foundation, Switzerland, and the Budai Foundation, Lichtenstein, to JHB (grant no. 310030_144152), and the Mäxi Foundation to O.M. We are grateful to Prof. B. Coller, New York, for the generous gift of the 6D1 antibody against human GpIb. We thank the Center for Microscopy and Image Analysis at the University of Zurich (ZMB).

Autorship Contributions

Stivala and Sorrentino designed the study, performed the experiments and analysed the data. Stivala wrote the manuscript with input from S. Sorrentino, OM and JHB. SG helped in processing samples and revised the manuscript. OM helped in designing the cryo-ET experiments. JHB designed the study with inputs from NB, GC and TL.

Disclosure of Conflicts of Interest

The authors have no conflicts of interest to declare.

References

1. Canobbio I, Balduini C, Torti M. Signalling through the platelet glycoprotein Ib-V-IX complex. Cell Signal. 2004;16(12):1329–1344.

2. Bergmeier W, Piffath CL, Goerge T, et al. The role of platelet adhesion receptor GPIbalpha far exceeds that of its main ligand, von Willebrand factor, in arterial thrombosis. Proc Natl Acad Sci U S A. 2006;103(45):16900–16905.

3. Englund GD, Bodnar RJ, Li Z, Ruggeri ZM, Du X. Regulation of von Willebrand factor binding to the platelet glycoprotein Ib-IX by a membrane skeleton-dependent inside-out signal. J Biol Chem. 2001;276(20):16952–16959.

4. Yago T, Lou J, Wu T, et al. Platelet glycoprotein Ibα forms catch bonds with human WT vWF but not with type 2B von Willebrand disease vWF. J Clin Invest. 2008;118(9):3195–3207.

5. Fu H, Jiang Y, Yang D, Scheiflinger F, Wong WP, Springer TA. Flow-induced elongation of von Willebrand factor precedes tension-dependent activation. Nat Commun. 2017;8(1):324.

6. Butera D, Passam F, Ju L, et al. Autoregulation of von Willebrand factor function by a disulfide bond switch. Sci Adv. 2018;4(2):eaaq1477.

7. Sakariassen KS, Orning L, Turitto VT. The impact of blood shear rate on arterial thrombus formation. Futur Sci OA. 2015;1(4):FSO30.

8. Casa LDC, Deaton DH, Ku DN. Role of high shear rate in thrombosis. J Vasc Surg. 2015;61(4):1068–1080.

9. Winnik S, Lohmann C, Richter EK, et al. Dietary α-linolenic acid diminishes experimental atherogenesis and restricts T cell-driven inflammation. Eur Heart J. 2011;32(20):2573-2584.

10. Holy EW, Forestier M, Richter EK, et al. Dietary α-linolenic acid inhibits arterial thrombus formation, tissue factor expression, and platelet activation. Arterioscler Thromb Vasc Biol. 2011;31(8):1772–1780.

11. Campos H, Baylin A, Willett WC. Alpha-linolenic acid and risk of nonfatal acute myocardial infarction. Circulation. 2008;118(4):339–345.

12. Sala-Vila A, Guasch-Ferré M, Hu FB, et al. Dietary α-Linolenic Acid, Marine ω-3 Fatty Acids, and Mortality in a Population With High Fish Consumption: Findings From the PREvención con DIeta MEDiterránea (PREDIMED) Study. J Am Heart Assoc. 2016;5(1):1–12.

13. Guallar E, Sanz-Gallardo MI, van't Veer P, et al. Mercury, fish oils, and the risk of myocardial infarction. N Engl J Med. 2002;347(22):1747–1754.

14. Mozaffarian D, Rimm EB. Fish intake, contaminants, and human health: evaluating the risks and the benefits. JAMA. 2006;296(15):1885–1899.

15. Morris MC, Brockman J, Schneider JA, et al. Association of Seafood Consumption, Brain Mercury Level, and APOEε4 Status With Brain Neuropathology in Older

Adults. JAMA. 2016;60612(5):489–497.

16. Shaikh SR, Jolly CA, Chapkin RS. n-3 Polyunsaturated fatty acids exert immunomodulatory effects on lymphocytes by targeting plasma membrane molecular organization. Mol Aspects Med. 2012;33(1):46–54.

17. Shaikh SR, Rockett BD, Salameh M, Carraway K. Docosahexaenoic acid modifies the clustering and size of lipid rafts and the lateral organization and surface expression of MHC class I of EL4 cells. J Nutr. 2009;139(9):1632–1639.

18. Chen W, Jump DB, Esselman WJ, Busik J V. Inhibition of cytokine signaling in human retinal endothelial cells through modification of caveolae/lipid rafts by docosahexaenoic acid. Invest Ophthalmol Vis Sci 2007;48(1):18–26.

19. Stivala S, Reiner MF, Lohmann C, Lüscher TF, Matter CM, Beer JH. Dietary α-linolenic acid increases the platelet count in ApoE-/- mice by reducing clearance. Blood. 2013;122(6):1026–1033.

20. Shrimpton CN, Borthakur G, Larrucea S, Cruz MA, Dong J-F, Lopez JA. Localization of the Adhesion Receptor Glycoprotein Ib-IX-V Complex to Lipid Rafts Is Required for Platelet Adhesion and Activation. J Exp Med. 2002;196(8):1057–1066.

21. Munday a D, Gaus K, López J a. The platelet glycoprotein Ib-IX-V complex anchors lipid rafts to the membrane skeleton: implications for activation-dependent cytoskeletal translocation of signaling molecules. J Thromb Haemost. 2010;8(1):163–172.

22. Gitz E, Koopman CD, Giannas A, et al. Platelet interaction with von Willebrand factor is enhanced by shear-induced clustering of glycoprotein Ibα. Haematologica. 2013;98(11):1810–1818.

23. Harper CR, Edwards MJ, DeFilipis AP, Jacobson TA. Flaxseed oil increases the plasma concentrations of cardioprotective (n-3) fatty acids in humans. J Nutr. 2006;136(1):83–87.

24. Canobbio I, Trionfini P, Guidetti GF, Balduini C, Torti M. Targeting of the small GTPase Rap2b, but not Rap1b, to lipid rafts is promoted by palmitoylation at Cys176 and Cys177 and is required for efficient protein activation in human platelets. Cell Signal. 2008;20(9):1662–1670.

25. Bodin S, Tronchère H, Payrastre B. Lipid rafts are critical membrane domains in blood platelet activation processes. Biochim Biophys Acta. 2003;1610(2):247–257.

26. Gousset K, Wolkers WF, Tsvetkova NM, et al. Evidence for a physiological role for membrane rafts in human platelets. J Cell Physiol. 2002;190(1):117–128.

27. Sorrentino S, Studt JD, Horev MB, Medalia O, Sapra KT. Toward correlating structure and mechanics of platelets. Cell Adhes Migr. 2016;10(5):568–575.

28. Lewandrowski U, Wortelkamp S, Lohrig K, et al. Platelet membrane proteomics: a novel repository for functional research. Blood. 2009;114(1):e10–e19.

29. Turgay Y, Eibauer M, Goldman AE, et al. The molecular architecture of lamins in somatic cells. Nature. 2017;543(7644):261–264.

30. Albert CM, Oh K, Whang W, et al. Dietary alpha-linolenic acid intake and risk of sudden cardiac death and coronary heart disease. Circulation. 2005;112(21):3232–3238.

31. Djoussé L, Arnett DK, Carr JJ, et al. Dietary linolenic acid is inversely associated with calcified atherosclerotic plaque in the coronary arteries: the National Heart, Lung, and Blood Institute Family Heart Study. Circulation. 2005;111(22):2921–2926.

32. Bark DL, Ku DN. Wall shear over high degree stenoses pertinent to atherothrombosis. J Biomech. 2010;43(15):2970–2977.

33. Strony J, Beaudoin A, Brands D, Adelman B. Analysis of shear stress and hemodynamic factors in a model of coronary artery stenosis and thrombosis. Am J Physiol. 1993;265(5 Pt 2):H1787-1796.

34. Reininger AJ, Heijnen HFG, Schumann H, Specht HM, Schramm W, Ruggeri ZM. Mechanism of platelet adhesion to von Willebrand factor and microparticle formation under high shear stress. Blood. 2006;107(9):3537–3545.

35. Webb Y, Hermida-Matsumoto L, Resh MD. Inhibition of protein palmitoylation, raft localization, and T cell signaling by 2-bromopalmitate and polyunsaturated fatty acids. J Biol Chem. 2000;275(1):261–270.

Legends to figures

Figure 1 Platelet adhesion to vWF is inhibited by alpha-linolenic acid. EDTA-blood pre-incubated with vehicle or alpha-linolenic acid (ALA) for 1 hour was perfused on vWF at high-shear rate and platelet adhesion monitored by fluorescence microscopy. Platelet-covered area measured at the end of the perfusion (A) or every minute during the perfusion (B) was significantly reduced by the ALA treatment (n=6, p=0.0039). The first time point in B corresponds to 5 seconds after start of the flow. (C) Single platelet rolling velocity measurements showed an increased speed in the ALA-treated samples, and a correspondingly increased distance until firm adhesion (D) (n=6, p=0.04 for C and p=0.0009 for D). (E) representative projection images of a vehicle- or ALA-treated sample showing single platelets rolling over vWF. (F) Membrane cholesterol depletion by pre-incubation of EDTA-blood with methyl-beta cyclodextrin completely abolished platelet adhesion to vWF (n=6, $p<0.0001$).

Figure 2. High-shear induces vWF binding in PRP but not in washed platelets. (A) Washed platelets were exposed to high-shear flow and analysed for GpIb abundance by flow cytometry, revealing no difference between vehicle and ALA-treated platelets (n=3). MFI= mean fluorescence intensity. (B) PRP was either left untreated or exposed to high-shear flow, and platelet-bound vWF analysed by flow cytometry. In both vehicle and ALA samples, high-shear flow induced vWF binding, as shown by a 3-fold increase compared to unsheared samples (n=3, $p<0.05$). (C) Exposing washed platelets (WP) to high-shear flow does not lead to vWF binding; addition of exogenous human vWF before shear exposure results in a robust binding (n=3).

Figure 3. **High-shear induces a local rearrangement of GpIb as revealed by cryo-ET.** Immunogold labeling (A-C) and neighborhood analysis (E-G) for the control (A, E), shear activated (B, F) and ALA-treated shear activated (C, G) platelets. (A-C): projection images (~70 nm in thickness) obtained from tomograms of platelet where GpIb alpha has been immunogold labeled. The labeling detection has been done with protein G conjugated to 6 nm gold (to make the gold detection easier, the gold has been labeled with red circles). With yellow arrows, we indicated crowded neighborhood occurring in the pictures. All the projections have the same scale and the scale bar in A is 100 nm. (E-G): analysis of the immunogold labeling. The 3D coordinates of the 6 nm gold particles from 6 tomograms for each condition were selected and the distance to the "neighboring receptors" within a radius of 50 nm were calculated. The number of neighbors each receptor has is depicted in the histogram. (D): integrin αIIbβ3 immunogold labeling was performed on spread platelets and the same neighbouring analysis performed (H).

Figure 4. Comparison of GpIb labeling by super-resolution microscopy and cryo-electron tomography reveals a similar receptor distribution. (A) The GpIb receptors in shear-activated platelets were labeled and images by GSD as described in the Material and Methods. (B) In order to compare the localization of the receptor by cryo-ET and GSD, a synthetic model of platelet perimeter was generated by merging 17 tomograms from the gold-labeled platelets. The gold particle coordinates from the synthetic platelets where filtered to the same resolution of the GSD (20 nm), represented here in red. White arrowheads indicate local clustering areas. Scale bar: 2.5 μm for both A and B.

Figure 5. Analysis of GpIb distribution by total internal reflection microscopy (TIRF). Superresolution analysis of GpIb in vehicle (A), ALA (B) or MbCD (C) platelets shows no detectable differences in the distribution of the receptor as measured by the particle size (D). Scale bar: 2.5 μm.

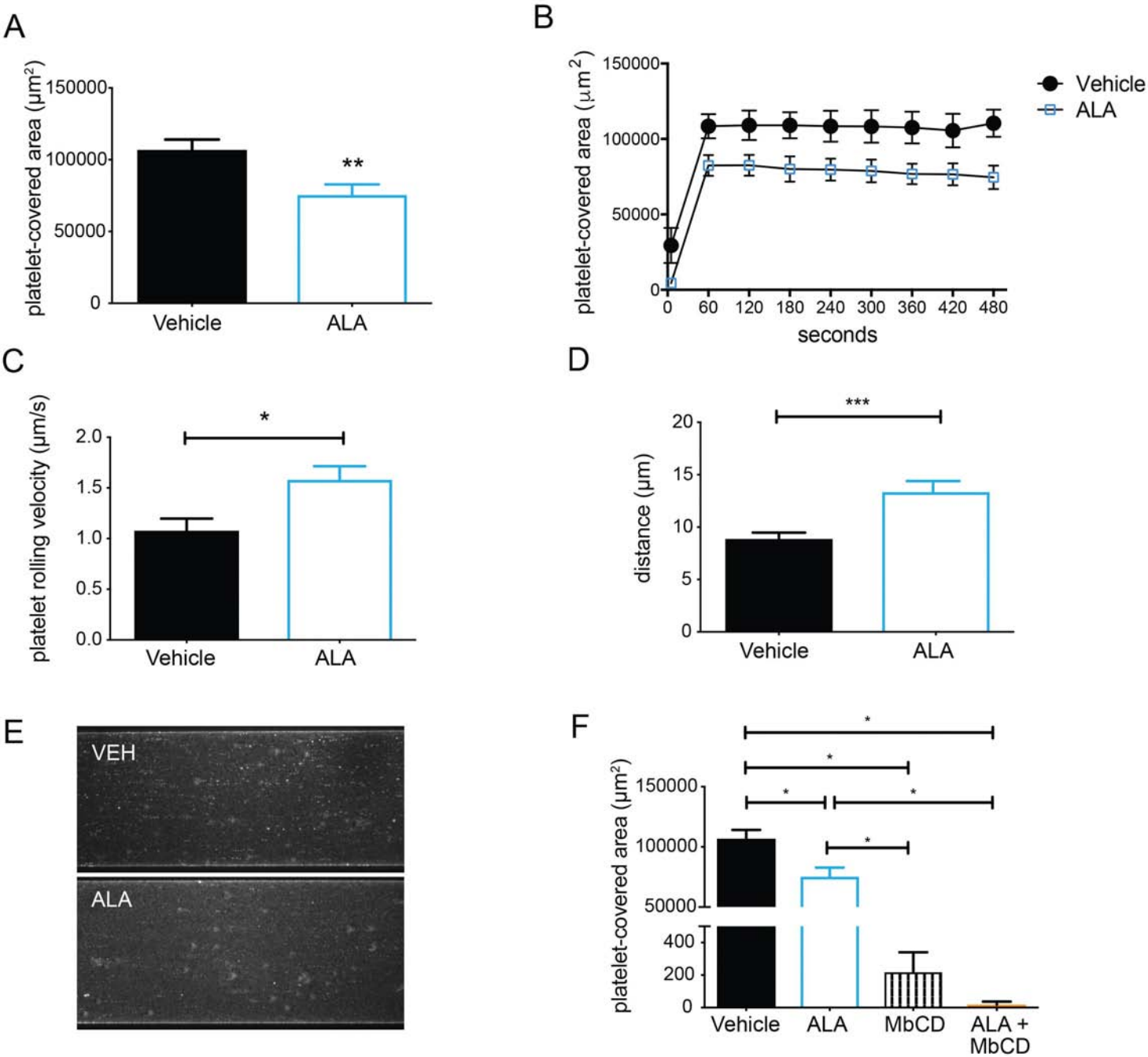
A
platelet-covered area (μm²)
150000
100000
50000
0
**
Vehicle
ALA
B
platelet-covered area (μm²)
150000
100000
50000
0
0
60
120
180
240
300
360
420
480
seconds
Vehicle
ALA
C
platelet rolling velocity (μm/s)
2.0
1.5
1.0
0.5
0.0
*
Vehicle
ALA
D
distance (μm)
20
15
10
5
0
***
Vehicle
ALA
E
VEH
ALA
F
platelet-covered area (μm²)
150000
100000
50000
400
200
0
*
*
*
*
*
Vehicle
ALA
MbCD
ALA + MbCD

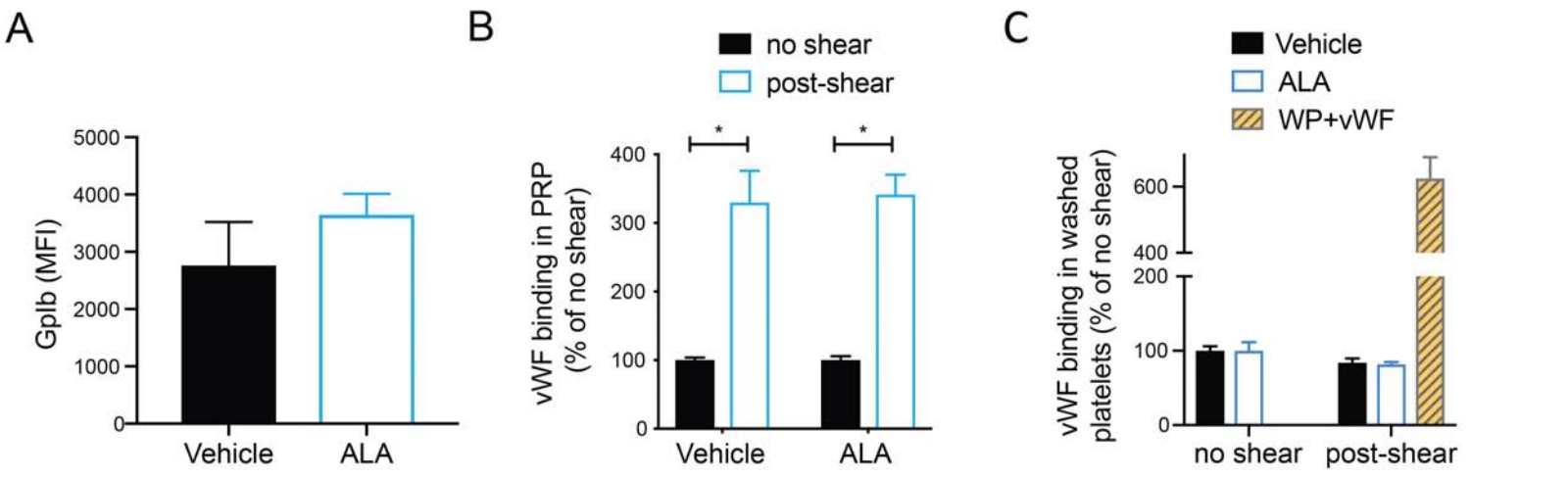
A
GpIb (MFI)
5000
4000
3000
2000
1000
0
Vehicle
ALA
B
no shear
post-shear
vWF binding in PRP
(% of no shear)
400
300
200
100
0
*
*
Vehicle
ALA
C
Vehicle
ALA
WP+vWF
vWF binding in washed
platelets (% of no shear)
600
400
200
100
0
no shear
post-shear

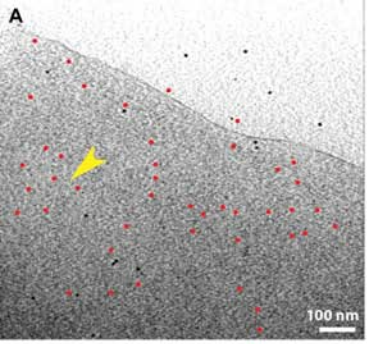
A
100 nm

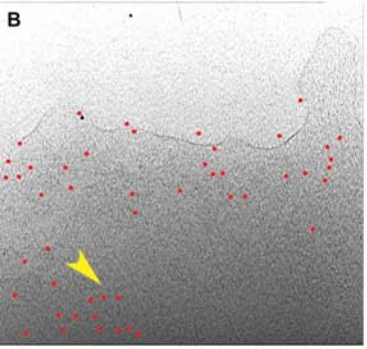
B

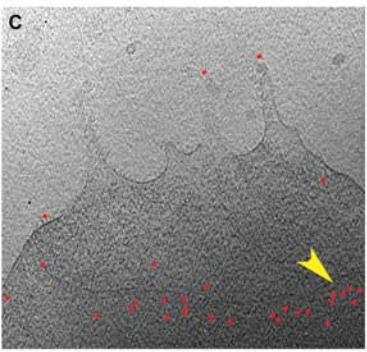
C

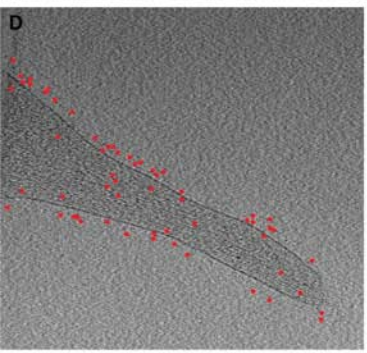
D

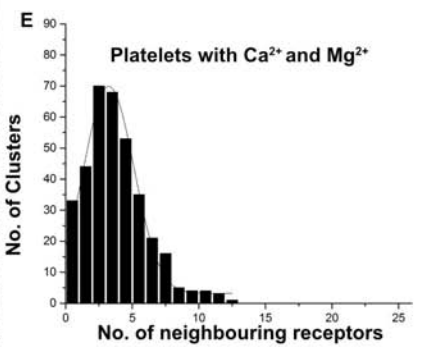
E
Platelets with Ca2+ and Mg2+
No. of Clusters
No. of neighbouring receptors

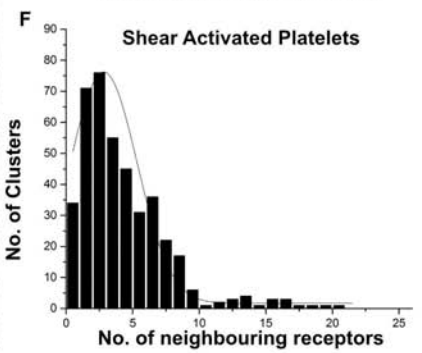
F
Shear Activated Platelets
No. of Clusters
No. of neighbouring receptors

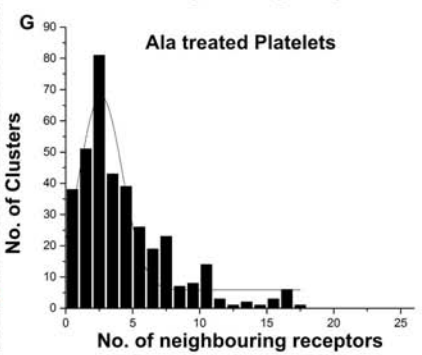
G
Ala treated Platelets
No. of Clusters
No. of neighbouring receptors

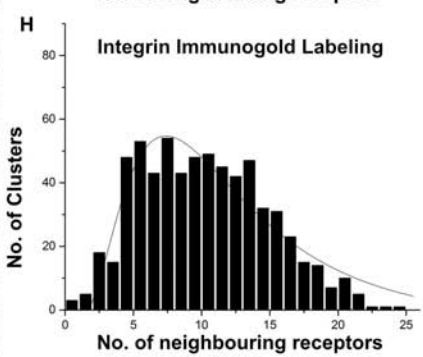
H
Integrin Immunogold Labeling
No. of Clusters
No. of neighbouring receptors

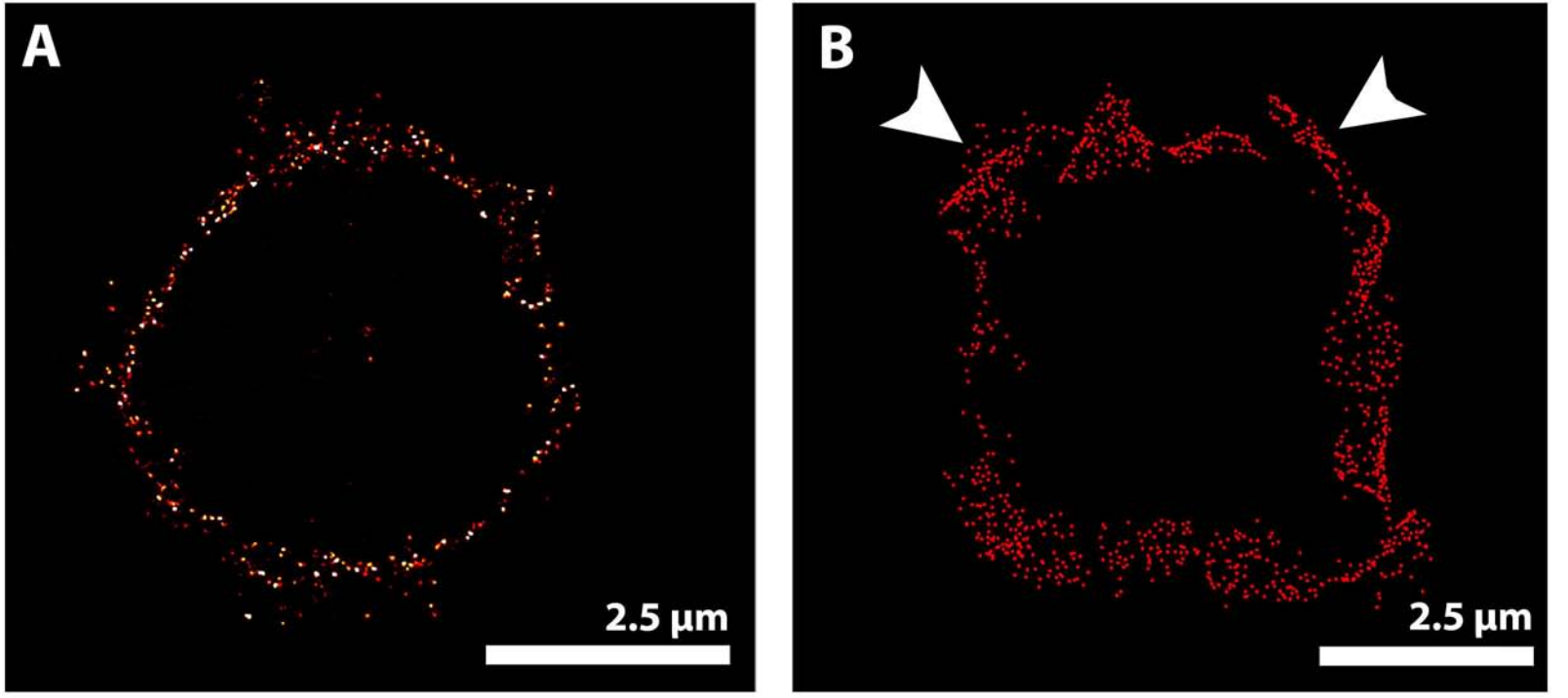
A
2.5 µm
B
2.5 µm

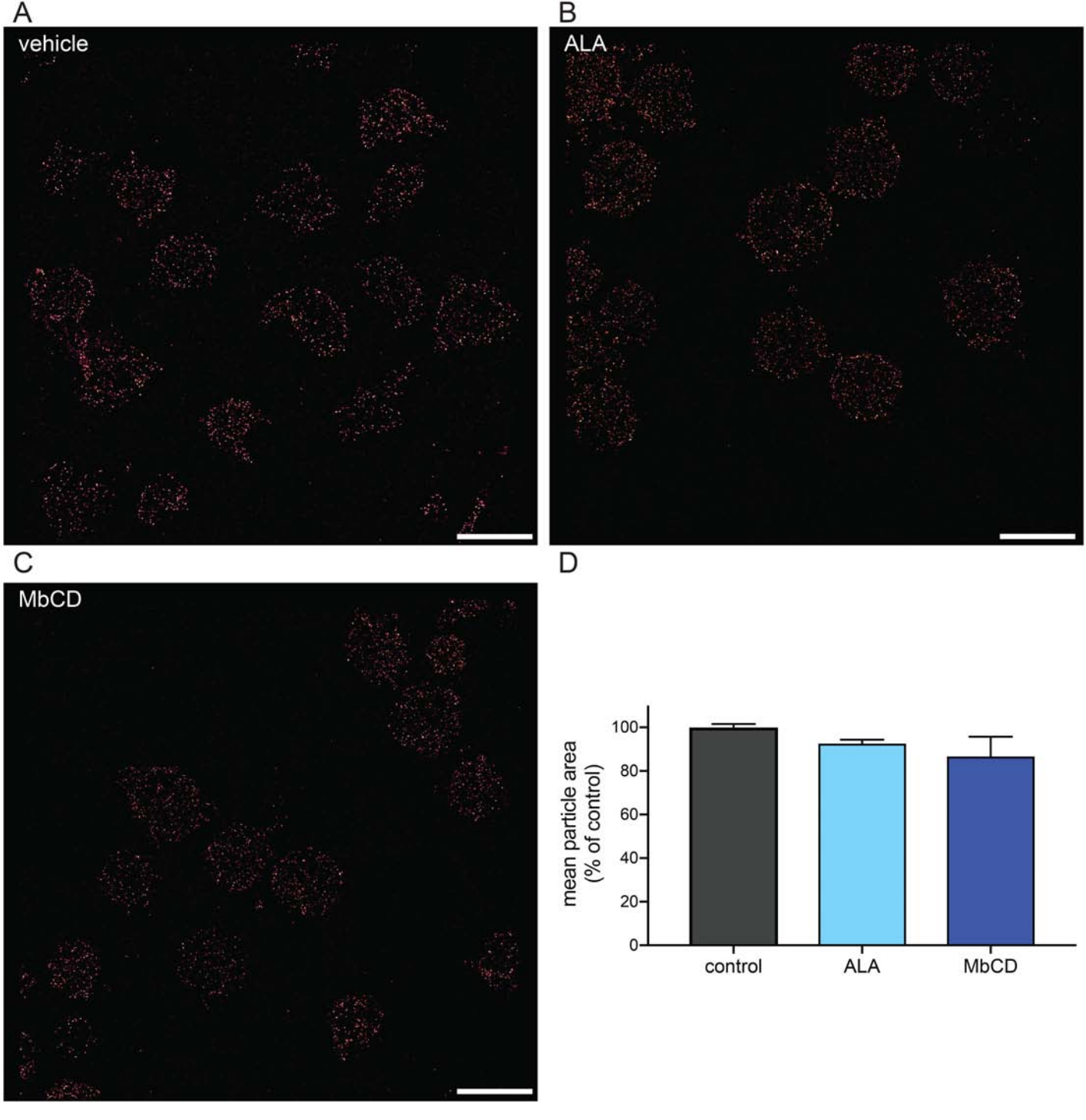
A
vehicle
B
ALA
C
MbCD
D
mean particle area
(% of control)
100
80
60
40
20
0
control
ALA
MbCD

Supplementary Data

Platelet isolation and cholesterol depletion

Shearing of platelets was performed on washed platelets isolated by centrifuging platelet rich plasma (PRP) at 340 RCF for 10 min in the presence of 1 μM PGE1, followed by washing with platelet wash buffer (26 mM Na_2HPO_4, 140 mM NaCl, pH=7.2) and resuspension in Tyrode's buffer (137 mM NaCl, 12 mM $NaHCO_3$, 5.5 mM glucose, 2 mM KCl, 1 mM $MgCl_2$, 2 mM $CaCl_2$, 0.3 mM Na_2HPO_4, pH=7.4). One hundred microliters of washed platelets were subjected to shear stress for 1 min at a rate of 10'000 s^{-1} (55 dynes/cm^2) in a cone-and-plate viscometer (CAP2000; Brookfield Inc., Middleboro, Massachusetts, USA). This shear rate has been shown to occur at clinically relevant 60–80% arterial stenoses[1]. The stainless-steel surfaces of the viscometer were precoated with 0.1% BSA in Tyrode's buffer for 1 min.
For platelet-rich plasma (PRP) isolation, blood was centrifuged at 200 RCF for 15 minutes, and PRP carefully removed and centrifuged again to remove contaminating leukocytes and erythrocytes. Cholesterol depletion of platelets was obtained by incubation of PRP with 10 mM methyl-beta cyclodextrin (Santa Cruz, US) at 37°C for 30 minutes.

Platelet adhesion to vWF under high-shear flow

Twenty-four-well plates were coated with human vWF (100 ug/ml, Hematologic Technologies Inc., US) for 1 hour, then washed with PBS +Ca^{2+} and Mg^{2+} and blocked with 0,1% BSA in PBS for 10 minutes. EDTA-anticoagulated blood was incubated with 30 μM ALA, EPA or stearic acid (from Cayman Chemical, US) or the same volume of vehicle (ethanol), at room temperature for 1 hour under gentle shaking, and platelets were concomitantly fluorescently labelled with calcein (4 μM final concentration, Enzo Life Science, US). Platelet adhesion was monitored on an inverted microscope (Leica Leitz DM IRB) with a 10x/0.22 NA objective and FITC filter by capturing images for 5 minutes after applying a flow of 100 dyn/cm^2 to the blood. Platelet-covered area (fluorescent area) was calculated in the region of view with the Bioflux software and expressed as μm^2.

Immunofluorescence staining for Ground State Depletion (GSD) microscopy

Samples were stained with a mouse anti-human GpIb-Alexa 647 antibody (MBL International, Woburn, US) in PBS for 2 hours at r.t., followed by 3 washes and post-fixation with 4% PFA. For integrin αIIbβ3 staining, platelets were incubated with a mouse anti-human primary

antibody (Abcam, Cambridge, UK) in PBS for 1 hour at room temperature, followed by 3 washes in PBS and a secondary antibody (donkey anti-mouse Alexa 647, Jackson Immunoresearch, West Grove, PA, USA) for 1 hour at room temperature[2]. Ground state depletion (GSD) and total internal reflection fluorescence (TIRF) microscopy was performed on a Leica SR GSD 3D microscope with a HCPL Apo 160x/1.43 NA objective. For imaging, samples were mounted in 200 mM phosphate buffer, pH=8.0, containing 15 mM cysteamine hydrochloride, 0.5 mg/ml glucose oxidase and 40 ug/ml catalase (all from Sigma-Aldrich, Buchs, Switzerland) as oxygen scavenging solution. We acquired 40'000 images exciting with a 633-nm laser and a 7.07 msec exposure; for TIRF, the penetration depth was 110 nm. Particle analysis in TIRF was performed with Fiji[3]. Alexa 647 switches reversibly between the on and off state, therefore, each Alexa 647 molecule might generate multiple detected events.

Cryo-electron tomography

Washed platelets obtained as described in "Platelet isolation" were seeded on gold grids coated with a Silicon mesh (R 1/4, 200 mesh, Quantifoli, Jena Germany). In case of shear activation, platelets were exposed to 10'000 s^{-1} shear rate for 1 min before being seeded. If indicated, platelets were treated with ALA as described above. Platelets were allowed to adhere on the grids for maximum 10 min and then they were fixed with 4% formaldhehyde for 5 min at room temperature. The time where platelets were allowed to spread on the grids was chosen based on a previous publication showing that GpIb clustering was stable for up to 10 minutes post-shear[4]. The EM grids were incubated in 0.05 M glycine/PBS for 15 min at room temperature to inactivate aldehyde groups present after fixation. Next, samples were blocked in blocking solution (5% BSA/0.1% cold water fish skin gelatin/PBS; Aurion) for 30 min at room temperature and subsequently washed 3 × 5 min with the incubation solution (0.2% BSA-c/PBS; Aurion). Immunogold analysis was performed using anti-human GpIb antibody (6D1, generous gift from B. Coller, Rockefeller University NY) at a dilution of 1:100 in the incubation solution (0.2% BSA-c/PBS; Aurion) for 1 hour at room temperature. Next, the EM grids were washed 6 × 5 min at room temperature with incubation solution (0.2% BSA-c/PBS; Aurion) before treatment with the gold conjugate (protein G coupled to 6 nm gold; Aurion) in incubation solution at a dilution of 1:40 for 2 hours at room temperature. After extensive washing (6 × 5 min at room temperature) with the incubation solution, fiducial markers of 10 nm were added (Aurion) and then the EM grids were plunge frozen in liquid ethane. Data acquisition was performed using an FEI Titan Krios transmission electron microscope equipped with a quantum energy filter and a K2-Summit direct electron detector (Gatan,

Pleasanton, USA). Tomograms were acquired with a magnification of 42,000× corresponding to a pixel size of 0.34 nm. The cumulative electron dose was ~80 electrons per ångström^2. To analyze the GpIb receptor density, the 3D coordinates of the 6 nm gold were selected using the tom_volxyz software from the TOM toolbox software package[5]. We used MATLAB to search how many 6 nm gold particles were present in a radius of 50 nm (using the selected coordinates) for each of the gold particle. The amount of gold particles found with this procedure is called: number of neighbors. In case of the negative control, no neighbors were found (data not shown). The plots of the distribution for number of neighbors for each receptor and the statistical analysis were performed using the OriginLab software. In particular, for the peak analysis we used the peak Fitting tool from OriginLab. For the analysis, we used 28 tomograms of platelets incubated with Calcium and Magnesium-containing buffer, 11 tomograms from shear activated platelets, 3 tomograms from the negative control. The analysis shown in the paper were performed on 6 tomograms for each condition.

Comparison between immunogold labeling and immunofluorescent data

The comparison between the GSD and the cryo-EM data was performed described previously[6]. Briefly, 25 tomograms were projected into 2-D images and assembled such to mimic the membrane of a platelet. Then the xy coordinates of GpIb (6 nm gold particles) were extracted and represented as 2D Gaussian functions with a full width at half maximum of 20 nm using MATLAB. Finally, these images were colored in red using Fiji[3].

References

1. Holme PA, Ørvim U, Hamers MJAG, et al. Shear-Induced Platelet Activation and Platelet Microparticle Formation at Blood Flow Conditions as in Arteries With a Severe Stenosis. Arterioscler Thromb Vasc Biol 1997;17(4):646 LP – 653.
2. Tamir A, Sorrentino S, Motahedeh S, et al. The macromolecular architecture of platelet-derived microparticles. J Struct Biol 2016;193(3):181–187.
3. Schindelin J, Arganda-Carreras I, Frise E, et al. Fiji: an open-source platform for biological-image analysis. Nat Methods 2012;9(7):676–682.
4. Gitz E, Koopman CD, Giannas A, et al. Platelet interaction with von Willebrand factor is enhanced by shear-induced clustering of glycoprotein Ibα. Haematologica 2013;98(11):1810–1818.
5. Nickell S, Förster F, Linaroudis A, et al. TOM software toolbox: acquisition and analysis for electron tomography. J Struct Biol 2005;149(3):227–234.
6. Turgay Y, Eibauer M, Goldman AE, et al. The molecular architecture of lamins in somatic cells. Nature 2017;543(7644):261–264.

Supplementary Figure 1 – Original cryo-ET images of the platelets displayed in Figure 2

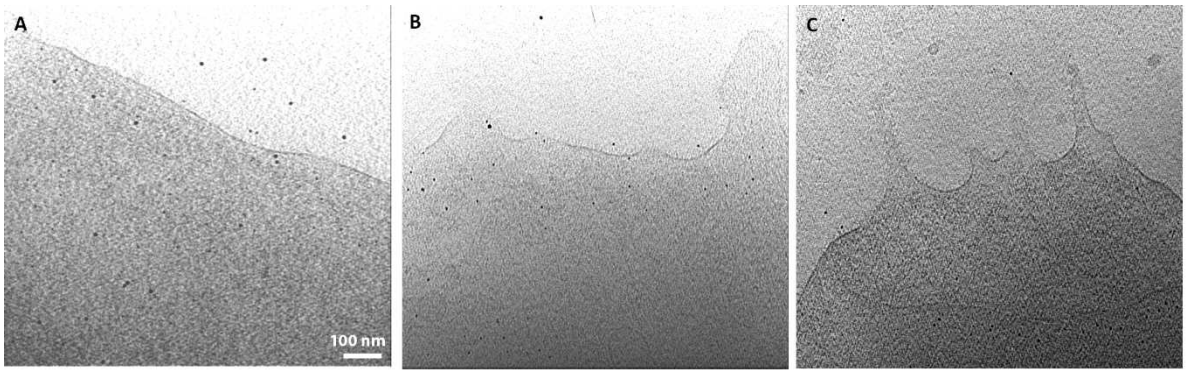

Figure S1. Original projection images from Fig. 2 where the 6 nm gold has not been labelled in red. The letter code has been kept the same.

Supplementary Figure 2 – Synthetic platelet, before and after filtering

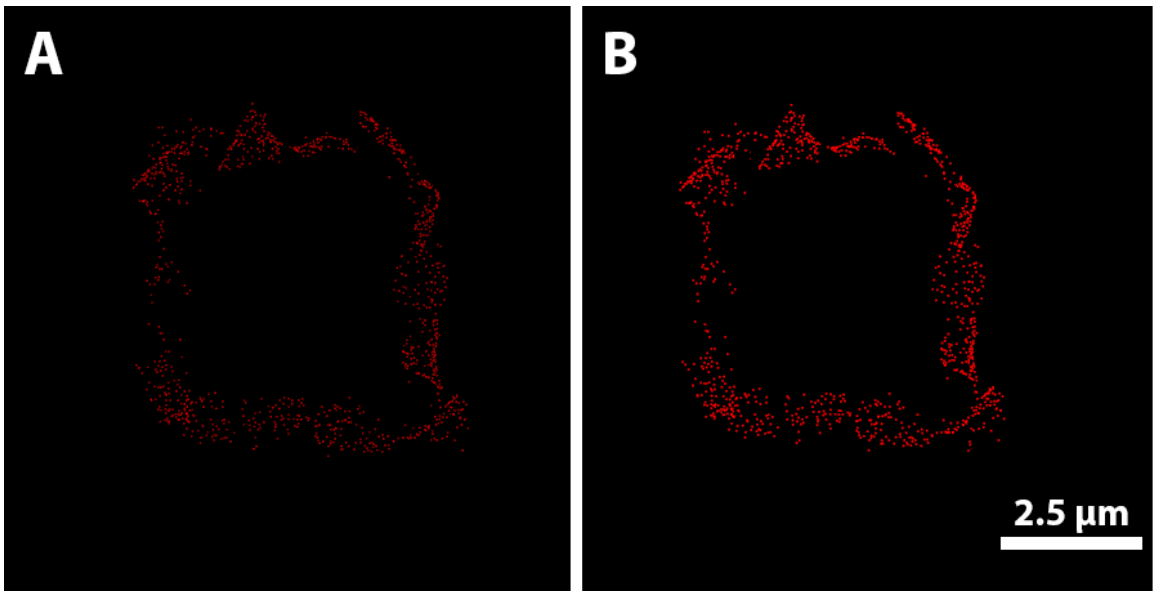

Figure S2. Synthetic platelet model. The coordinates of the antibody labelled GpIb (6 nm gold particles) from 17 tomograms represented as 2D Gaussian functions with a full width at half maximum of 10 nm (in A) and 20 nm (in B) using MATLAB. We choose to show the image from B in Figure 4 in order to match the resolution for GSD.

Supplementary Figure 3 – Ground state depletion (GSD) microscopy on integrin αIIbβ3

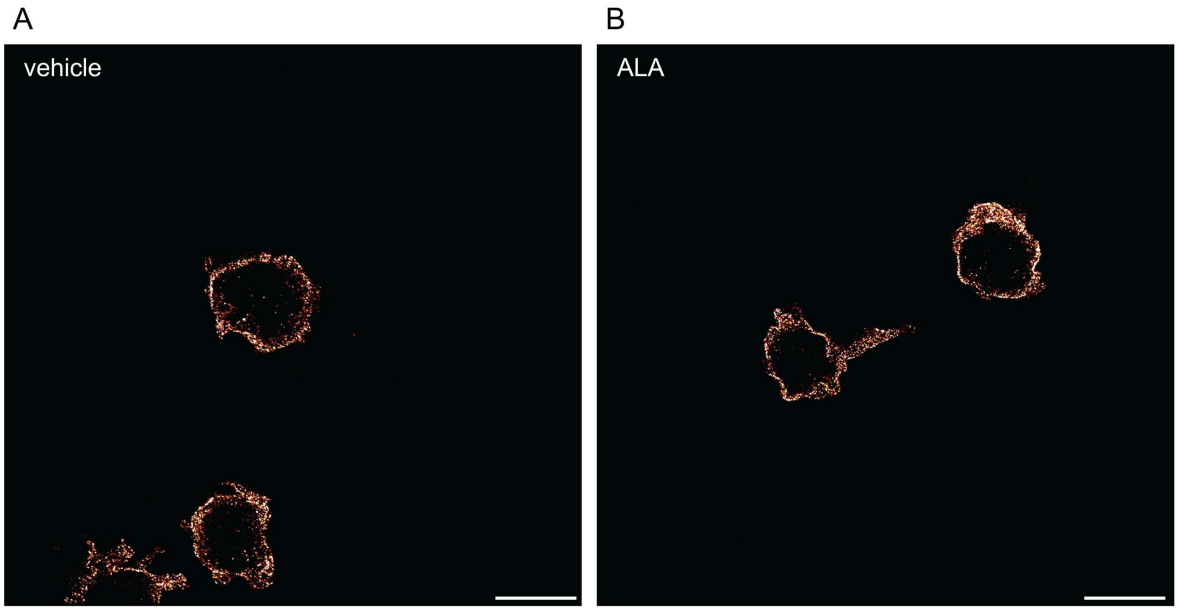

Figure S3. Superresolution microscopy by GSD on vehicle (A) and ALA-treated (B) platelets shows no difference in the distribution of the integrin αIIbβ3. Scale bar: 3 μm.

Supplementary Figure 4 – Inhibition of platelet adhesion to vWF by the long-chain n3-FA eicosapentaenoic acid (EPA)

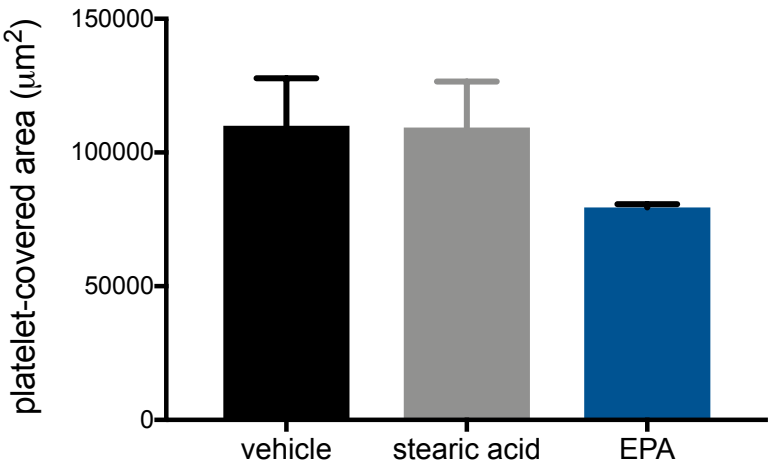

Figure S4. Adhesion experiments under high-shear flow show that the marine-derived n3-FA EPA has a similar inhibitory effect on the platelet-covered area on vWF, whereas the saturated fatty acid stearic acid has no effect on platelet adhesion (n=3).

Supplementary video 1. Platelet adhesion to vWF under high-shear flow after treatment with vehicle (0.1% ethanol).

Supplementary video 2. Platelet adhesion to vWF under high-shear flow after whole blood treatment with 30 μM alpha-linolenic acid.